Predicting Mass Transfer in Packed Columns*

Reinhard Billet and Michael Schultes**

Countercurrent-flow columns are widely used in production processes in the chemical industry and their application in ecological engineering is of increasing importance. A theoretical model is presented here that allows mass transfer to be described in terms of packing geometry and physical properties which influence the gas-liquid or vapour-liquid systems in absorption, desorption and rectification columns. The relationships derived from the model can be applied to all countercurrent-flow columns, regardless of whether the packing has been dumped at random or arranged in a geometric pattern.

1 Mass Transfer in the Liquid Phase

The geometry and dimensions of modern packings are the main parameters that govern the flow of various phases and thus also the column efficiency. The liquid must flow in the form of a thin film and be distributed as uniformly as possible over the entire cross-section of the column in order to ensure large throughputs, effective mass transfer and moderate pressure drops. The surface of the packing should be wetted as much as possible and the countercurrent flow of gas should also be uniformly distributed over the column cross-section. Thus, the factors that govern the fluid dynamics and mass transfer of a column are the physical properties of the system, its capacity range and the shape and structure of the packing [1].

The efficiency of a packing is influenced by the length of flow path l_τ which has to be traversed before the surface of the liquid in contact with the gas is renewed. Since the liquid is continually remixed at the points of contact with the packing, according to Higbie, the mass transfer in the liquid phase occurs by non-steady state diffusion, Eq. (1). D_L is the diffusion coefficient of the transferring component and the time τ_L necessary for the renewal of interfacial area is determined by Eq. (2) with liquid hold-up h_L, length of flow path l_τ and liquid load u_L [2][1].

$$\beta_L = \frac{2}{\sqrt{\pi}} \sqrt{D_L \frac{1}{\tau_L}} \,, \tag{1}$$

$$\tau_L = h_L l_\tau \frac{1}{u_L} \,. \tag{2}$$

If the packing is regarded as a large number of channels through which the liquid of density ϱ_L and viscosity η_L flows as a film with a local velocity $\bar{u}_{L,s}$ countercurrent to a stream of gas, liquid flow can be described by the equilibrium of forces, Eq. (3), provided that the forces of inertia are negligible. This equation applies at any given point $0 \le s \le s_0$ in the laminar liquid film [1 – 3].

$$\frac{\mathrm{d}\left(\eta_i \dfrac{\mathrm{d}\bar{u}_{L,s}}{\mathrm{d}s}\right)}{\mathrm{d}s} = -\varrho_L g \,. \tag{3}$$

Gravity and shear forces in the film are maintained at equilibrium with the frictional forces by the shear stress τ_V in the gas or vapour flow at the surface of the film, Eq. (4). In Eq. (4), ϱ_V is the gas density, $\bar{u}_V$ the average effective gas velocity and ψ_L the drag coefficient for the gas-liquid or vapour-liquid countercurrent flow.

$$\tau_V = -\tfrac{1}{2} \psi_L \varrho_V \bar{u}_V^2 \,. \tag{4}$$

Integration of Eq. (3) and substitution of the frictional force of the gas, acting at the surface of the liquid, by Eq. (4), lead theoretically to Eq. (5), valid for the liquid hold-up h_L at and below the loading point [2 – 4]. In Eq. (5), u_L is the liquid load based on the column cross-section and a the total surface area of the packing.

$$h_L = \left(12 \frac{1}{g} \frac{\eta_L}{\varrho_L} u_L a^2\right)^{1/3} \,. \tag{5}$$

Combining Eqs (1), (2) and (5) gives rise to Eq. (6) for the volumetric mass transfer coefficient $\beta_L a_{Ph}$ and Eq. (7) for the height of a transfer unit HTU_L on the liquid-side, with C_L being a constant, characteristic of the shape and structure of the packing [2, 5, 6].

$$\beta_L a_{Ph} = C_L \left(\frac{g}{\nu_L}\right)^{1/6} \left(\frac{D_L}{l_\tau}\right)^{1/2} a^{2/3} u_L^{1/3} \left(\frac{a_{Ph}}{a}\right) \,, \tag{6}$$

$$HTU_L = \frac{1}{C_L} \left(\frac{\nu_L}{g}\right)^{1/6} \left(\frac{l_\tau}{D_L}\right)^{1/2} \left(\frac{u_L}{a}\right)^{2/3} \left(\frac{a}{a_{Ph}}\right) \,. \tag{7}$$

* Summary of papers presented at AIChE 1988 National Spring Meeting, New Orleans, LA/USA, and AIChE 1988 Annual Meeting, Washington, D.C./USA.

** Prof. Dr.-Ing. R. Billet and Dr.-Ing. M. Schultes, Lehrstuhl für Thermische Stofftrennverfahren, Ruhruniv. Bochum, Universitätsstr. 150, D-4630 Bochum 1.

1) List of symbols at the end of the paper.

0930-7516/93/0102-0001 $5.00+.25/0

2 Mass Transfer in the Gas Phase

The theoretical model is based on the assumption that the gas flows through the packing in different directions, passing mixing zones as well as those where mass transfer occurs. The theoretical time interval τ_V required for the renewal of the contact area between the phases is defined by the length of the flow path l_τ, the superficial gas velocity u_V, the void fraction ε and the liquid hold-up h_L, cf. Eq. (8).

$$\tau_V = (\varepsilon - h_L) l_\tau \frac{1}{u_V} \quad . \tag{8}$$

The time of contact τ_V corresponding to the flow path l_τ is comparatively short in conventional packed beds, and mass transfer takes place in a very thin sublayer. Therefore, it can be assumed that, in analogy to the formulation of Higbie, mass transfer in the gas phase, the law of non-steady state diffusion described by Eq. (9) also follows. This equation contains the coefficient of diffusion D_V for the solute in the gas phase.

$$\beta_V = \frac{2}{\sqrt{\pi}} \sqrt{D_V \frac{1}{\tau_V}} \quad . \tag{9}$$

Together with Eqs (5) and (8), Eq. (9) gives rise to Eq. (10) for the volumetric mass transfer coefficient $\beta_V a_{Ph}$ and to Eq. (11) for the height of a transfer unit HTU_V on the gas-side, in which the exponents $m = 3/4$ and $n = 1/3$ on the gas Reynolds number $u_V/(a\nu_V)$ and the Schmidt number ν_V/D_V allow the best correlation of the test results [6, 7].

$$\beta_V a_{Ph} = C_V \frac{1}{(\varepsilon - h_L)^{1/2}} \frac{a^{3/2}}{l_\tau^{1/2}} D_V \left(\frac{u_V}{a\nu_V}\right)^m \left(\frac{\nu_V}{D_V}\right)^n \left(\frac{a_{Ph}}{a}\right) , \tag{10}$$

$$HTU_V = \frac{1}{C_V} (\varepsilon - h_L)^{1/2} \frac{l_\tau^{1/2}}{a^{3/2}} \frac{u_V}{D_V} \left(\frac{a\nu_V}{u_V}\right)^m \left(\frac{D_V}{\nu_V}\right)^n \left(\frac{a}{a_{Ph}}\right) . \tag{11}$$

In these equations, a_{Ph} is the effective interfacial area for mass transfer and C_V a constant, characteristic of the shape and structure of the packing, which has to be determined experimentally.

3 Results of Experiments on Absorption and Desorption

Results of mass transfer measurements performed in the Department of Thermal Separation Processes at Bochum University and those taken from literature [8 – 37] were systematically evaluated to check the mathematical model thus described. They embraced 31 different systems, cf. Tables 1 a – 1 c, and 67 different types and sizes of packings, cf. Tables 2a and 2b. The total number of measurements evaluated was about 2600.

A dimensional analysis of the influencing parameters showed that the volumetric mass transfer coefficients could be determined most accurately if the characteristic length of the flow path l_τ were described in terms of the hydraulic diameter d_h, cf. Eq. (12), and the ratio a_{Ph}/a were given by Eq. (13) [6].

$$l_\tau = d_h = 4\frac{\varepsilon}{a} , \tag{12}$$

$$\frac{a_{Ph}}{a} = 1.5 (a d_h)^{-0.5} \left(\frac{u_L d_h}{\nu_L}\right)^{-0.2} \left(\frac{u_L^2 \varrho_L d_h}{\sigma_L}\right)^{0.75} \left(\frac{u_L^2}{g d_h}\right)^{-0.45} ,$$

$$= 1.5 (a d_h)^{-0.5} Re_L^{-0.2} We_L^{0.75} Fr_L^{-0.45} . \tag{13}$$

Thus, the factors governing the ratio of the interfacial to the geometric surface area are the density ϱ_L, kinematic viscosity ν_L and surface tension σ_L of the liquid, area of the unwetted packing a, hydraulic diameter d_h and liquid load u_L.

Table 1a. Physical properties of investigated systems with mass transfer resistance mainly in the liquid phase.

Systems with liquid phase resistance	T [K]	ϱ_L [kg/m³]	$\nu_L \cdot 10^6$ [m²/s]	$\sigma_L \cdot 10^3$ [kg/s²]	$D_L \cdot 10^9$ [m²/s]	Sc_L [–]
Carbon dioxide/water	288	1003	1.14	74.0	1.59	713
Carbon dioxide/methanol	298	788	0.70	23.8	3.63	193
Carbon dioxide/ buffer solution 1	298	1157	1.22	72.0	1.40	871
Carbon dioxide/ buffer solution 2	298	1237	1.66	72.0	1.40	1186
Carbon dioxide/ 1.78 molal NaCl solution	298	1040	1.04	76.0	1.63	641
Carbon dioxide-water/air	293	997	0.97	72.4	1.82	535
Carbon dioxide-air/water	293	998	1.00	72.7	1.82	549
Oxygen-water/air	296	996	0.94	72.0	2.40	391
Chlorine-air/water	294	997	0.98	72.0	1.33	741

Table 1b. Physical properties of investigated systems with mass transfer resistance mainly in the gas phase.

Systems with gas phase resistance	T [K]	ϱ_V [kg/m³]	$\nu_V \cdot 10^6$ [m²/s]	$\sigma_L \cdot 10^3$ [kg/s²]	$D_V \cdot 10^6$ [m²/s]	Sc_V [–]
Air/water	293	1.188	15.1	72.5	24.6	0.612
Air/methanol	300	1.162	15.6	22.4	16.5	0.950
Air/benzene	300	1.162	15.6	27.4	9.1	1.720
Air/ethyl *n*-butyrate	300	1.162	15.6	21.8	7.4	2.122
Helium/water	303	0.159	126.2	71.3	87.4	1.443
Freon 12/water	303	4.797	2.9	71.3	10.9	0.247
Ammonia-nitrogen/water	289	1.167	14.9	72.8	24.4	0.609
Ammonia-oxygen/water	298	1.291	15.9	72.2	14.7	1.085
Ammonia-air/4% H_2SO_4 in water	294	1.180	15.2	59.4	24.0	0.632
Sulphur dioxide-air/ 1.78 molal NaOH in water	294	1.190	15.1	54.6	12.3	1.224
Sulphur dioxide-Freon 12/ 3 molal NaOH in water	303	4.800	2.4	70.9	5.0	0.480
Chlorine-air/ 2 molal NaOH in water	303	1.150	15.9	70.9	13.3	1.200
Acetone-nitrogen/water	289	1.166	14.9	72.7	10.8	1.378

Table 1c. Physical properties of investigated systems with mass transfer resistance in both gas and liquid phases.

Systems with gas and liquid phase resistance	T [K]	ϱ_V [kg/m^3]	$\nu_V \cdot 10^6$ [m^2/s]	$D_V \cdot 10^6$ [m^2/s]	Sc_V [–]	ϱ_L [kg/m^3]	$\nu_L \cdot 10^6$ [m^2/s]	$\sigma_L \cdot 10^3$ [kg/s^2]	$D_L \cdot 10^9$ [m^2/s]	Sc_L [–]
Ammonia-air/water	293	1.188	15.1	23.8	0.633	999	1.03	72.7	1.72	597
Ammonia-propane/water	301	1.763	4.7	14.9	0.317	996	0.84	72.0	2.01	418
Ammonia-Freon 12/water	295	4.929	2.2	12.2	0.185	998	0.96	72.4	1.79	536
Sulphur dioxide-air/water	303	1.150	15.9	13.1	1.220	989	0.99	70.0	1.87	530
Sulphur dioxide-oxygen/water	297	1.297	15.6	12.9	1.208	998	0.92	72.3	1.66	556
Acetone-air/water	300	1.162	15.6	10.8	1.452	997	0.86	72.1	1.18	728
Methanol-air/water	300	1.162	15.6	16.5	0.950	997	0.86	72.1	1.44	600
Ethanol-air/water	298	1.168	15.5	12.4	1.246	997	0.89	72.2	1.09	819
Carbon dioxide-air/1 molal NaOH in water	293	1.187	15.1	15.4	0.980	1043	1.20	75.0	1.77	678

Table 2a. Characteristic data of dumped packings and constants C_L and C_V in Eqs (6), (7) and (10), (11), respectively.

Dumped packing	Material	Size	N [1/m^3]	a [m^2/m^3]	E [m^3/m^3]	C_L	C_V
		50 mm*	6242	112.6	0.951	1.192	0.410
	Metal	38 mm	15772	149.6	0.952	1.227	0.341
		35 mm*	19517	139.4	0.965	1.012	
		25 mm*	53900	223.5	0.954	1.440	0.336
Pall rings							
		50 mm*	6765	111.1	0.919	1.239	0.368
	Plastic	35 mm*	17000	151.1	0.906	0.856	0.380
		25 mm*	52300	225.0	0.887	0.905	0.446
	Ceramic	50 mm*	6215	116.5	0.783	1.227	0.415
Ralu rings	Plastic	50 mm	5770	95.2	0.938	1.520	0.303
		50 mm, hydr.	5720	95.2	0.939	1.481	0.341
		50 mm	7330	86.8	0.947	1.080	0.322
		35 mm*	17450	141.8	0.944	0.756	0.425
NOR PAC rings	Plastic	25 mm, type A	52356	211.0	0.951	0.862	
		25 mm, type B	50000	202.0	0.953	0.883	0.366
		25 mm, type C	47619	192.0	0.922	0.888	
		25 mm, 10 webs*	48920	197.9	0.920	0.976	0.410
	Metal	50 mm	5000	92.3	0.977	1.168	0.408
		25 mm*	40790	202.9	0.962	1.641	0.402
		50 mm*	6815	117.1	0.925	1.487	0.345
Hiflow rings	Plastic	50 mm, hydr.*	6890	118.4	0.925	1.553	0.369
		25 mm*	46100	194.5	0.918	1.577	0.390
		50 mm	5120	89.7	0.809	1.377	0.379
	Ceramic	38 mm	13241	111.8	0.788	1.659	0.464
		20 mm, 4 webs	110741	261.2	0.779	1.744	0.465
Hilflow rings; Super	Plastic	50 mm	6050	82.0	0.942	1.219	0.342
TOP-Pac rings	Aluminium	50 mm	6871	105.5	0.956	1.326	0.389
		50 mm	5990	95.0	0.830	1.416	0.210
		38 mm	13275	118.0	0.680	1.536	0.230
		25 mm*	47700	190.0	0.680	1.361	0.412
	Ceramic	15 mm*	189091	312.0	0.690	1.276	0.401
		13 mm	378000	370.0	0.640	1.367	0.265
Raschig rings		10 mm	672000	440.0	0.650	1.303	0.272
		8 mm	1261000	550.0	0.650	1.210	
		6 mm	3022936	771.9	0.620	1.130	
	Carbon	25 mm	50599	202.2	0.720	1.379	0.471
		13 mm	378000	370.0	0.640	1.419	
VSP rings	Metal	50 mm, no. 2	7841	104.6	0.980	1.222	0.420
		25 mm, no. 1	33434	199.6	0.975	1.376	0.405

Table 2a. (continued)

Dumped packing	Material	Size	N [1/m³]	a [m²/m³]	E [m³/m³]	C_L	C_V
		80 mm, no. 3	2000	60.0	0.955	1.603	0.257
Envi Pac rings	Plastic	60 mm, no. 2	6800	98.4	0.961	1.522	0.296
		32 mm, no. 1	53000	138.9	0.936	1.517	0.459
		50 mm *	6278	121.0	0.966	1.721	0.302
	Metal	35 mm *	18200	155.0	0.967	1.412	0.390
Bialecki rings		25 mm *	48533	210.0	0.956	1.461	0.331
		25 mm	436096	419.5	0.901	1.431	0.288
	Plastic	50 mm	3900	100.0	0.972	1.798	
Tellerettes	Plastic	25 mm	37037	190.0	0.930	0.899	
Spheres	Glass	25 mm	66664	134.5	0.430	1.335	
		13 mm	561877	282.2	0.400	1.364	
		38 mm	24928	164.0	0.700	1.568	0.244
Berl saddles	Ceramic	25 mm	80080	260.0	0.680	1.246	0.387
		13 mm	691505	545.0	0.650	1.364	0.232
Intalox saddles	Ceramic	13 mm	730000	625.0	0.780	1.677	0.488

Abbr.: hydr. = hydrophilized; * = likewise investigated for rectification.

Table 2b. Characteristic data of regular packings and constants C_L and C_V in Eqs (6), (7) and (10), (11), respectively.

Regular packing	Material	Size	N [1/m³]	a [m²/m³]	E [m³/m³]	C_L [–]	C_V [–]
Pall rings	Ceramic	50 mm	7502	155.2	0.754	1.278	0.333
Hiflow rings	Plastic	50 mm	7640	131.3	0.916	1.374	
		50 mm, hydr.	8150	140.1	0.911	1.437	
Blalecki rings	Metal	35 mm	20736	176.6	0.945	1.405	0.377
Ralu pack	Metal	YC-250*		250.0	0.945	1.334	0.385
	Metal	250		250.0	0.975	0.983	0.270
Impulse packing		50		55.0	0.806	0.939	
	Ceramic	100		91.4	0.838	1.317	0.327
		100, n		102.7	0.816	1.170	0.383
	Metal	B1 – 200		200.0	0.979	0.971	0.390
		B1 – 300		300.0	0.930	1.165	0.422
Montz packing							
	Plastic	C1 – 200		200.0	0.954	1.006	0.412
		C2 – 200		200.0	0.900	0.739	
Euroform	Plastic	PN-110		110.0	0.936	0.973	0.167

Abbr.: hydr. = hydrophilized; n = new stacked; * = likewise investigated for rectification.

If the constants C_V and C_L of Eqs (6), (7) and (10), (11) are assigned to a specific packing, cf. Tables 2a and 2b, the mean relative deviations of the calculated mass transfer coefficients from the experimentally determined values for absorption and desorption processes are 8.3% for the liquid-side and 12.4% for the gas-side. This is evident from Figs 1 and 2.

4 Results of Rectification Experiments

During rectification, the physical properties of the liquid and vapour phases change along the height of the column. If the surface tension in the liquid phase varies from the top to the bottom of the column, surface tension gradients occur which influence the interfacial area of the liquid film. Systems with

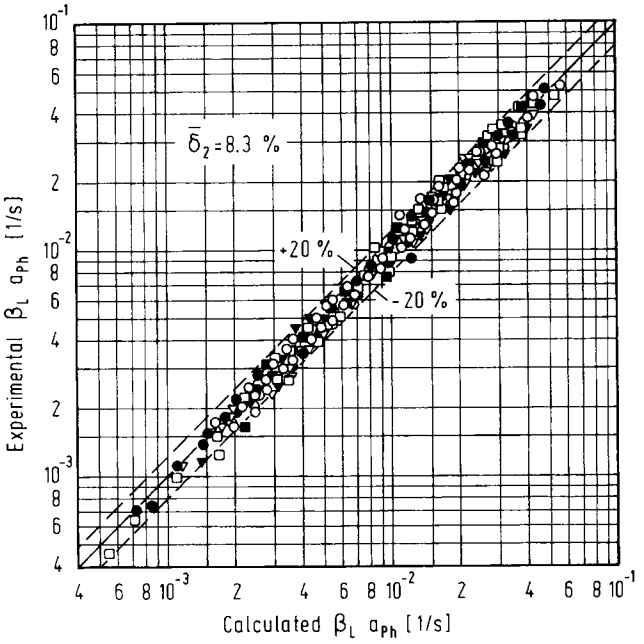

Fig. 1. Comparison of the volumetric mass transfer coefficient in the liquid phase, calculated from Eq. (6), with experimental results.

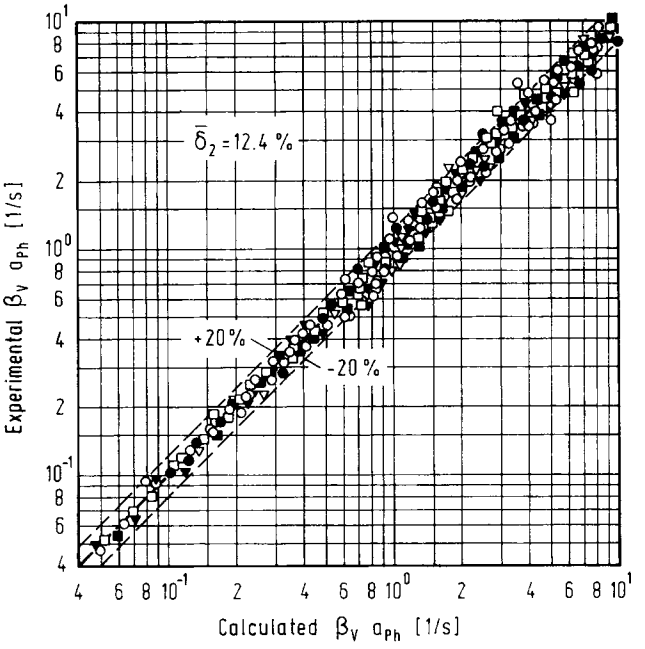

Fig. 2. Comparison of the volumetric mass transfer coefficient in the gas phase, calculated from Eq. (10), with experimental results.

increasing surface tension along the liquid flow path are referred to as positive systems whereas, for negative systems, surface tension decreases. If it remains more or less constant throughout the process, the system is regarded as neutral [35].

The shear stress caused by the surface tension gradient τ_σ, cf. Eq. (14), is in equilibrium with the shear stress in the liquid film τ_N [38, 39], cf. Eq. (15), which theoretically leads to the Marangoni number Ma_L, defined by Eq. (16) [6]. In Eq. (14), H is the height coordinate from the top to the bottom of the column and x the mole fraction of the more volatile component in the liquid phase. The Marangoni number describes the differential change $d\sigma_L/dx$ in surface tension along the column, with the composition of the liquid phase determined by a concentration difference Δx from the bulk of the liquid to the surface.

$$\tau_\sigma = \frac{d\sigma_L}{dH} = \frac{d\sigma_L}{dx}\frac{dx}{dH}\,, \tag{14}$$

$$\tau_N = \eta_L \frac{d\bar{u}_{L,s}}{ds}\,, \tag{15}$$

$$Ma_L = \frac{d\sigma_L}{dx}\frac{\Delta x}{D_L \eta_L a}\,. \tag{16}$$

Since the liquid phase equilibrium concentration at the surface x_{Ph} cannot be measured, Δx has to be calculated by Eq. (17) from the mass transfer resistance distribution on the liquid-side HTU_L/HTU_{OL}, cf. Eqs (18) and (19), and the overall concentration difference $(x - x^*)$. The latter can be determined from the operating and equilibrium lines, cf. Fig. 3.

$$\Delta x = (x - x_{Ph}) = \frac{HTU_L}{HTU_{OL}}(x - x^*)\,, \tag{17}$$

$$\frac{HTU_L}{HTU_{OL}} = \frac{X}{1+X}\,, \tag{18}$$

$$X = \frac{C_V}{C_L} m_{yx} \frac{\tilde{M}_L}{\tilde{M}_V}\frac{\varrho_V}{\varrho_L}\frac{\nu_L^{1/6}}{\nu_V^{5/12}}\frac{D_V^{2/3}}{D_L^{1/2}}\frac{a^{1/2}}{g^{1/6}}\frac{1}{(\varepsilon - h_L)^{1/2}}\frac{u_V^{3/4}}{u_L^{1/3}}\,. \tag{19}$$

In Eqs (17), (18) and (19), HTU_{OL} is the height of an overall transfer unit on the liquid-side, m_{yx} the slope of the

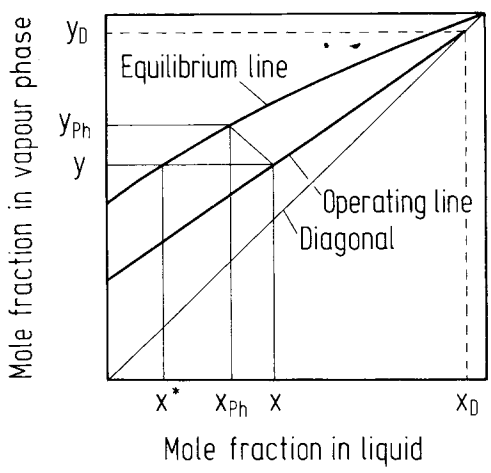

Fig. 3. Determination of liquid mole fraction x^* for calculating the concentration difference between liquid bulk and surface $(x - x_{Ph})$ by Eq. (17).

Table 3. Physical properties of systems investigated for rectification.

Systems for rectification	p_T [mbar]	T_s [K]	ϱ_V [kg/m³]	$\nu_V \cdot 10^6$ [m²/s]	$D_V \cdot 10^6$ [m²/s]	Sc_V [–]	ϱ_L [kg/m³]	$\nu_L \cdot 10^6$ [m²/s]	$\sigma_L \cdot 10^3$ [kg/s²]	$D_L \cdot 10^9$ [m²/s]	Sc_L [–]
Chlorobenzene/ethyl benzene[n]	33	314	0.140	52.4	64.8	0.809	956	0.59	28.5	2.33	255
Chlorobenzene/ethyl benzene[n]	67	329	0.268	28.7	35.8	0.803	941	0.52	26.9	2.85	181
Chlorobenzene/ethyl benzene[n]	133	345	0.510	15.8	19.9	0.793	926	0.45	25.1	3.50	128
Chlorobenzene/ethyl benzene[n]	267	364	0.967	8.8	11.1	0.791	908	0.39	23.2	4.33	89
Chlorobenzene/ethyl benzene[n]	533	385	1.827	4.9	6.3	0.785	887	0.34	21.1	5.41	62
Chlorobenzene/ethyl benzene[n]	1000	407	3.241	2.9	3.7	0.780	866	0.30	19.0	6.67	45
Toluene/*n*-octane[n]	103	321	0.373	19.1	21.0	0.908	779	0.53	23.1	2.33	195
Toluene/*n*-octane[n]	133	327	0.473	15.3	17.0	0.904	774	0.50	22.5	2.53	171
Toluene/*n*-octane[n]	267	345	0.900	8.5	9.5	0.894	758	0.43	20.7	3.18	118
Ethanol/water[p]	1000	352	1.294	8.2	14.5	0.567	787	0.53	25.7	3.42	82
Ethyl benzene/styrene[n]	133	350	0.483	15.9	19.9	0.798	835	0.45	21.0	3.64	123
trans-Decalin/cis-decalin[p]	13	336	0.066	105.8	120.0	0.881	846	1.24	26.0	1.04	1019
Methanol/ethanol[n]	1000	343	1.303	8.4	9.1	0.929	739	0.54	17.2	4.75	113
1,2 Dichlorethane/toluene[n]	1000	365	3.200	3.2	4.0	0.806	968	0.35	22.3	4.86	70

Abbr.: n = negative system; p = positive system.

equilibrium curve and $\tilde{M}_L$ and $\tilde{M}_V$ the molar masses of the phases.

Test results obtained in rectification columns at BASF [36, 37] and the Department of Thermal Separation Processes at Bochum University indicate for negative systems a reduction of the effective interfacial area a_{Ph} while, for positive systems, the liquid film becomes stabilized. The total number of measurements that could be applied in these studies was 665, including 14 different rectification systems, cf. Table 3, and 20 types of packings, cf. Tables 2a and 2b. These evaluations led to Eq. (20) for describing the ratio a_{Ph}/a for negative systems and to Eq. (13) for positive or neutral systems, cf. Eq. (21) [6].

For negative systems:

$$\left(\frac{a_{Ph}}{a}\right)_{Rect.} = \left(\frac{a_{Ph}}{a}\right)_{Eq.\,(13)} (1 - 2.4 \times 10^{-4} |Ma_L|^{0.5}) \quad . \quad (20)$$

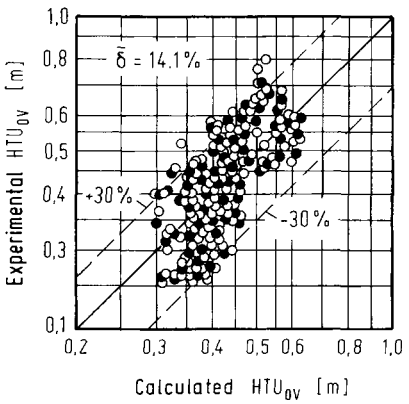

Fig. 4. Comparison of the overall mass transfer unit on the gas-side, calculated from Eqs (20) – (22), with experimental results.

For positive and neutral systems:

$$\left(\frac{a_{Ph}}{a}\right)_{Rect.} = \left(\frac{a_{Ph}}{a}\right)_{Eq.\,(13)} \quad . \quad (21)$$

For rectification columns, the calculated height of an overall mass transfer unit on the gas-side HTU_{OV}, cf. Eq. (22), can be compared with experimental results, if the constants C_V and C_L of Tables 2a and 2b are used. This is shown in Fig. 4. With an average relative deviation of 14.1%, the cited equations are again more accurate than the previous methods for calculating mass transfer in rectification.

$$HTU_{OV} = HTU_V + \lambda HTU_L \approx \frac{u_V}{\beta_V a_{Ph}} + \left(m_{yx}\frac{\dot{V}}{\dot{L}}\right)\frac{u_L}{\beta_L a_{Ph}} \quad . \quad (22)$$

5 Conclusions

The equations presented in this paper permit the prediction of mass transfer in absorption, desorption and rectification columns, up to the loading point. For the determination of mass transfer, physical properties, packing geometry and a specific shape constant for the packing, cf. Tables 2a and 2b, are required. Table 4 lists the capacity range, test facilities and physical properties relating to the investigations.

6 Example

Separation of ethyl benzene-styrene mixture into a top product containing x_D = 99 mol-% of ethyl benzene and a bottom product with x_W = 99.9 mol-% styrene. The process is operated under a reflux ratio of r = 6 and at a top pressure of 66.7 mbar, with an average relative volatility of

Table 4. Capacity range, test facilities and physical properties relating to the investigated systems.

Gas capacity factor	F_V [$m^{-1/2} kg^{1/2} s^{-1}$]	0.0029 – 2.773
Liquid load	u_L [$m^3/m^2 h$]	0.2563 – 118.20
Column diameter	d_s [m]	0.06 – 1.40
Column height	H [m]	0.152 – 3.950
Total surface area per unit volume	a [m^2/m^3]	55.00 – 711.9
Void fraction	ε [m^3/m^3]	0.40 – 0.98
Liquid density	ϱ_L [kg/m^3]	758 – 1237
Liquid viscosity	ν_L [m^2/s]	0.30 – 1.66
Liquid-side diffusion coefficient	D_L [m^2/s]	1.04 – 6.50
Surface tension	σ_L [kg/s^2]	17.2 – 74.0
Gas density	ϱ_V [kg/m^3]	0.066 – 4.929
Gas viscosity	ν_V [m^2/s]	2.2 – 126.2
Gas-side diffusion coefficient	D_V [m^2/s]	3.7 – 87.4
Schmidt number of liquid	Sc_L [–]	45 – 1186
Schmidt number of gas	Sc_V [–]	0.185 – 2.122
Number of investigated packings		67
Number of measurements for absorption and desorption		2605
Number of measurements for rectification		665
Investigated systems for absorption and desorption		31
Investigated systems for rectification		14

$\alpha = 1.37$. The column is filled with Montz sheet metal packing type B1 – 200. The height of an overall transfer unit on the gas-side HTU_{OV} has to be calculated.

The influence of the mixture's composition is taken into account by dividing into sections of height or concentration. The first section shall be defined by the liquid concentration from the top $x_D = 99$ mol-% to $x = 80$ mol-% with an average slope of the equilibrium line of $m_{yx} = 0.7737$.

The physical properties in this range are:

Molar mass of vapour	$\tilde{M}_V = 105.98$ kg/kmol
Molar mass of liquid	$\tilde{M}_L = 105.95$ kg/kmol
Density of vapour	$\varrho_V = 0.290$ kg/m³
Density of liquid	$\varrho_L = 840.1$ kg/m³
Viscosity of vapour	$\eta_V = 7.31 \times 10^{-6}$ kg/ms
Viscosity of liquid	$\eta_L = 0.426 \times 10^{-3}$ kg/ms
Diffusion coefficient in vapour	$D_V = 31.9 \times 10^{-6}$ m²/s
Diffusion coefficient in liquid	$D_L = 3.154 \times 10^{-9}$ m²/s
Surface tension of liquid	$\sigma_L = 24.01 \times 10^{-3}$ kg/s²

The characteristic data of packing and constants follow from Table 2b:

Total surface area per unit volume	$a = 200$ m²/m³
Relative void fraction	$\varepsilon = 0.979$ m³/m³
Constants	$C_L = 0.971$; $C_V = 0.390$

Operating conditions in the first section:

Vapour velocity	$u_V = 4.57$ m/s
Liquid load	$u_L = 1.36 \times 10^{-3}$ m³/m²s
Molar vapour flow rate	$\dot{V} = 423.96$ kmol/h
Molar liquid flow rate	$\dot{L} = 364.40$ kmol/h

The hydraulic diameter d_h and the liquid hold-up h_L are calculated from Eqs (12) and (5):

$$d_h = 4\frac{0.979}{200} = 0.01958 \text{ m} ,$$

$$h_L = \left(12\frac{0.426\times10^{-3}\times1.36\times10^{-3}\times200^2}{9.806\times840.1}\right)^{1/3}$$

$$= 0.032 \text{ m}^3/\text{m}^3 .$$

Since ethyl benzene-styrene is a negative system, cf. Table 3, a surface tension gradient is present. At the top of the column, $x_D = 99$ mol-%, the surface tension is $\sigma_L = 0.0248$ kg/s² and, for $x = 80$ mol-%, the surface tension is $\sigma_L = 0.0232$ kg/s². The gradient is therefore:

$$\frac{d\sigma_L}{dx} = \frac{\Delta\sigma_L}{\Delta x} = \frac{0.0248 - 0.0232}{0.99 - 0.80} = 0.00842 .$$

The driving concentration difference Δx can be determined according to Fig. 3 from the operating and equilibrium lines for the mean liquid concentration $x = (0.99 + 0.80)/2 = 0.985$ in the section. The vapour concentration corresponding to x results from the operating line at reflux ratio $r = 6$.

$$y = \frac{r}{r+1}x + \frac{x_D}{r+1} = \frac{6}{6+1}0.985 + \frac{0.99}{6+1} = 0.9086 ,$$

and the liquid concentration x^* in equilibrium with that of the vapour y is obtained from the equilibrium line at a relative volatility of $\alpha = 1.37$.

$$x^* = \frac{y}{\alpha - y(\alpha - 1)} = \frac{0.9086}{1.37 - 0.9086(1.37 - 1)} = 0.87884 .$$

The resistance distribution follows from Eqs (18) and (19):

$$\frac{HTU_L}{HTU_{OL}} = \frac{X}{1+X} ,$$

$$X = \frac{0.390\times0.7737\times105.95\times0.290(0.507\times10^{-6})^{1/6}(31.894\times10^{-6})^{2/3}}{0.971\times105.98\times840.1(25.168\times10^{-6})^{5/12}(3.154\times10^{-9})^{1/2}}\times$$

$$\times\frac{200^{1/12}\times4.57^{3/4}}{9.81^{1/6}(0.979-0.032)^{1/2}(1.36\times10^{-3})^{1/3}} = 0.437 ,$$

$$\frac{HTU_L}{HTU_{OL}} = \frac{0.437}{1+0.437} = 0.304 .$$

The driving concentration difference Δx from the bulk to the surface of the liquid

$$\Delta x = 0.304(0.985 - 0.87884) = 0.004913$$

allows the Marangoni number Ma_L to be calculated by Eq. (16):

$$Ma_L = 0.00842 \frac{0.004913}{3.154 \times 10^{-9} \times 0.426 \times 10^{-3} \times 200} =$$

$$= 1.53 \times 10^5 \ .$$

The interfacial area for mass transfer without the influence of Marangoni effects is calculated by Eq. (13):

$$\frac{a_{Ph}}{a} = 1.5(200 \times 0.01958)^{-0.5} \left(\frac{1.36 \times 10^{-3} \times 0.01958}{0.507 \times 10^{-6}} \right)^{-0.2} \times$$

$$\times \left(\frac{(1.36 \times 10^{-3})^2 840.1 \times 0.01958}{0.02401} \right)^{0.75} \times$$

$$\times \left(\frac{1.36 \times 10^{-3})^2}{9.806 \times 0.01958} \right)^{-0.45} = 0.416 \ .$$

Taking into consideration the effect of surface tension gradients, the interfacial area must be corrected by Eq. (20):

$$\frac{a_{Ph}}{a} = 0.416(1 - 2.4 \times 10^{-4} | 1.53 \times 10^5 |^{0.5}) = 0.377 \ .$$

The height of a transfer unit in the liquid phase is obtained from Eq. (7):

$$HTU_L = \frac{1}{0.971} \left(\frac{0.507 \times 10^{-6}}{9.806} \right)^{1/6} \left(\frac{0.01958}{3.15 \times 10^{-9}} \right)^{1/2} \times$$

$$\times \left(\frac{1.36 \times 10^{-3}}{200} \right)^{2/3} \left(\frac{1}{0.377} \right) = 0.149 \text{ m}$$

while that in the vapour phase is obtained from Eq. (11):

$$HTU_v = \frac{1}{0.390} (0.979 - 0.032)^{1/2} \frac{0.01958^{1/2}}{200^{3/2}} \frac{4.57}{31.9 \times 10^{-6}} \times$$

$$\times \left(\frac{200 \times 25.17 \times 10^{-6}}{4.57} \right)^{3/4} \left(\frac{31.9 \times 10^{-6}}{25.17 \times 10^{-6}} \right)^{1/3} \times$$

$$\times \left(\frac{1}{0.377} \right) = 0.307 \ .$$

The stripping factor λ relates the slopes of the equilibrium and operating lines

$$\lambda = m_{yx} \frac{\dot{V}}{\dot{L}} = 0.7737 \frac{423.96 \text{ kmol/h}}{363.40 \text{ kmol/h}} = 0.903$$

and allows the height of an overall transfer unit in the vapour phase HTU_{OV} to be calculated by Eq. (22):

$$HTU_{OV} = 0.307 + 0.903 \times 0.149 = 0.441 \text{ m} \ .$$

The number of theoretical stages per unit height n_{th}/H can be finally obtained as follows:

$$\frac{n_{th}}{H} = \frac{1}{HTU_{OV}} \frac{\lambda - 1}{\ln \lambda} = \frac{1}{0.441} \frac{0.903 - 1}{\ln 0.903} = 2.15 \text{ 1/m} \ .$$

Of course, this number is strictly valid only for ideal operating conditions and must be correspondingly scaled-up for a larger column.

Received: August 26, 1991 [CET 419]

Symbols used

a	[m^2/m^3]	Total surface area per unit packed volume
a_{Ph}	[m^2/m^3]	Effective interfacial area per unit packed volume
C	[–]	Constant
d_h	[m]	Hydraulic diameter
D	[m^2/s]	Diffusion coefficient of transferring component
g	[m/s^2]	Gravitational acceleration
H	[m]	Height
h_L	[m^3/m^3]	Liquid hold-up
HTU	[m]	Height of a mass transfer unit
HTU_O	[m]	Overall height of a mass transfer unit
$\dot{L}$	[kmol/h]	Molar flow rate of liquid
l_τ	[m]	Length of flow path
M	[kg/kmol]	Molar mass
m_{yx}	[kmol/kmol]	Slope of equilibrium line
n, m	[–]	Exponents
n_{th}	[–]	Number of theoretical stages
N	[$1/m^3$]	Packing density
r	[–]	Reflux ratio
s	[m]	Film thickness
T	[K]	Temperature
u_L	[m^3/m^2 s]	Liquid load
$\bar{u}_{L,s}$	[m/s]	Local liquid velocity
u_V	[m/s]	Superficial gas or vapour velocity
$\bar{u}_V$	[m/s]	Average effective gas or vapour velocity
$\dot{V}$	[kmol/h]	Molar flow rate of gas or vapour
β	[m/s]	Mass transfer coefficient
x	[kmol/kmol]	Mole fraction in liquid phase
y	[kmol/kmol]	Mole fraction in gas or vapour phase
α	[–]	Relative volatility
β	[m/s]	Mass transfer coefficient
δ	[%]	Relative error
ε	[m^3/m^3]	Void fraction
η	[kg/m s]	Viscosity
λ	[–]	Stripping factor
ν	[m^2/s]	Kinematic viscosity
ϱ	[kg/m^3]	Density
σ	[kg/s^2]	Surface tension
τ	[s]	Duration of contact
τ	[kg/m s^2]	Shear stress
ψ	[–]	Drag coefficient

Dimensionless numbers

$Fr_L = \frac{u_L^2}{g d_h}$	Froude number of liquid

$Ma_L = \frac{d\sigma_L}{dx}\frac{\Delta x}{D_L \eta_L a}$ Marangoni number

$Re_L = \frac{u_L d_h}{\nu_L}$ Reynolds number of liquid

$Re_V = \frac{u_V}{\nu_V a}$ Reynolds number of gas or vapour

$Sc_L = \frac{\nu_L}{D_L}$ Schmidt number of liquid

$Sc_V = \frac{\nu_V}{D_V}$ Schmidt number of gas or vapour

$We_L = \frac{u_L^2 \varrho_L d_h}{\sigma_L}$ Weber number of liquid

Subscripts

D	Top product
L	Liquid
o	Surface
Ph	Interface
s	Film thickness
V	Vapour
W	Bottom product

References

[1] Billet, R., *Chem. Eng Technol. 11* (1988) No. 3, pp. 139 – 148.
[2] Billet, R., *Festschrift der Fakultät für Maschinenbau*, Ruhr-Univ. Bochum 1983, pp. 24 – 31.
[3] Billet, R., *Inst. Chem. Eng Symp. Ser.* (1987) No. 104, pp. A171 – A182.
[4] Billet, R., Schultes, M., *Inst. Chem. Eng Symp. Ser.* (1987) No. 104, pp. B255 – B266.
[5] Billet, R., Schultes, M., *Paper at AIChE Meeting*, 1988, New Orleans.
[6] Schultes, M., *Thesis*, Ruhr-Univ. Bochum 1990, *Fortschr. Ber. VDI Z. 3* (1990) No. 230.
[7] Billet, R., Schultes, M., *Paper at AIChE Meeting*, 1988, Washington.
[8] Deed, D.W., Schutz, P.W., Drew, T.B., *Ind. Eng Chem. 39* (1947) No. 6, pp. 766 – 774.
[9] Hikita, H., Kataoka, T., Nakanishi, K., *Kagaku Kogaku 24* (1960) pp. 2 – 8.
[10] Houston, R.W., Walker, C.A., *Ind. Eng Chem. 42* (1950) No. 6, pp. 1105 – 1112.
[11] Hutchings, L.E., Stutzman, L.F., Koch, H.A., *Chem. Eng Prog. 45* (1949) No. 4, pp. 253 – 268.
[12] Joosten, G.E.H., Danckwerts, P.V., *Chem. Eng Sci. 28* (1973) pp. 453 – 461.
[13] Kim, J.H., *Thesis*, Ruhr-Univ. Bochum 1986.
[14] Kolev, N., *Verfahrenstechnik (Mainz)* (1969) No. 3, pp. 241 – 243.
[15] Lynch, E.J., Wilke, C.R., *AIChE J.* (1955) No. 1, pp. 9 – 19.
[16] Mohunta, D.M., Vaidyanathan, A.S., Ladda, G.S., *The First national heat and mass transfer conference*, Indian Institute of Technology, Madras, December 1971, Paper No. HMT-59-71, pp. 65 – 78.
[17] Molstad, M.C., Abbey, R.G., Thompson, A.R., McKinney, J.F., *Trans. Am. Inst. Chem. Eng 38* (1942) pp. 410 – 434.
[18] Molstad, M.C., Parsly, L.F., *Chem. Eng Prog. 46* (1950) No. 1, pp. 20 – 28.
[19] Onda, K., Sada, E., Murase, Y., *AIChE J. 5* (1959) No. 2, pp. 235 – 239.
[20] Onda, K., Okamota, T., Honda, H., *Kagaku-Kogaku 24* (1960) pp. 490 – 493.
[21] Onda, K., Sada, E., Saito, M., *Kagaku-Kogaku 25* (1961) pp. 820 – 829.
[22] Onda, K., Sada, E., Kido, C., Kawatake, S., *Kagaku-Kogaku* 30 (1966) pp. 226 – 229.
[23] Onda, K., Takeuchi, H., Okumoto, Y., *J. Chem. Eng Jpn* (1968) No. 1, pp. 56 – 62.
[24] Richards, G.M., Ratcliff, G.A., Danckwerts, P.V., *Chem. Eng Sci. 19* (1964) pp. 325 – 328.
[25] Sherwood, T.K., Holloway, F.A.L., *Chem. Eng Prog. 36* (1940) pp. 21 – 37.
[26] Sherwood, T.K., Holloway, F.A.L., *Chem. Eng Prog. 36* (1940) pp. 39 – 70.
[27] Sherwood, T.K., Pigford, R.L., *Absorption and extraction*, McGraw-Hill, New York 1952.
[28] Shulman, H.L., DeGouff, J.J., *Ind. Eng Chem. 44* (1916) No. 8, pp. 1915 – 1922.
[29] Surosky, A.E., Dodge, B.F., *Ind. Eng Chem. 42* (1950) No. 6, pp. 1112 – 1119.
[30] Vidwans, A.D., Sharma, M.M., *Chem. Eng Sci. 22* (1967) pp. 673 – 684.
[31] Vivian, J.E., Whitney, R.P., *Chem. Eng Prog. 43* (1947) No. 12, pp. 691 – 702.
[32] Whitney, R.P., Vivian, J.E., *Chem. Eng Prog. 45* (1949) No. 5, pp. 323 – 337.
[33] Yilmaz, T., *Chem.-Ing.-Tech. 45* (1973) No. 5, pp. 253 – 259.
[34] Yoshida, F., Koyanagi, T., *Ind. Eng Chem. 50* (1958) No. 3, pp. 365 – 374.
[35] Zuiderweg, F.J., Harmens, A., *Chem. Eng Sci. 9* (1958) No. 2/3, pp. 89 – 103.
[36] Billet, R., *Chem. Eng Prog. 63* (1967) No. 9, pp. 53 – 65.
[37] Billet, R., *Distillation Engineering*, Chemical Publishing Company, New York 1979.
[38] Drinkenburg, A.A.H., *Inst. Chem. Eng Symp. Ser.* (1987) No. 104, pp. B179 – B191.
[39] Brauer, H., *Stoffaustausch einschließlich chemischer Reaktionen*, Verlag Sauerländer, Aarau 1971.